Functional characterisation of banana (*Musa* spp.) 2-oxoglutarate-dependent dioxygenases involved in flavonoid biosynthesis

Short title: banana flavonoid 2-ODDs

Authors:

Mareike Busche[1], Christopher Acatay[1], Stefan Martens[2], Bernd Weisshaar[1], Ralf Stracke[1]*

[1] Genetics and Genomics of Plants, Faculty of Biology, Bielefeld University, 33615 Bielefeld, Germany

[2] Fondazione Edmund Mach, Research and Innovation Centre, San Michele All' Adige, TN, Italy

*Corresponding author:

Ralf Stracke

ralf.stracke@uni-bielefeld.de

Keywords: banana, specialised metabolites, flavanone 3-hydroxylases, flavonol synthase, anthocyanidin synthase

Abstract

Bananas (*Musa*) are non-grass, monocotyledonous, perennial plants that are well-known for their edible fruits. Their cultivation provides food security and employment opportunities in many countries. Banana fruits contain high levels of minerals and phytochemicals, including flavonoids, which are beneficial for human nutrition. To broaden the knowledge on flavonoid biosynthesis in this major crop plant, we aimed to identify and functionally characterise selected structural genes encoding 2-oxoglutarate-dependent dioxygenases, involved in the formation of the flavonoid aglycon.

Musa candidates genes predicted to encode flavanone 3-hydroxylase (F3H), flavonol synthase (FLS) and anthocyanidin synthase (ANS) were assayed. Enzymatic functionalities of the recombinant proteins were confirmed *in vivo* using bioconversion assays. Moreover, transgenic analyses in corresponding *Arabidopsis thaliana* mutants showed that *MusaF3H*, *MusaFLS* and *MusaANS* were able to complement the respective loss-of-function phenotypes, thus verifying functionality of the enzymes *in planta*.

Knowledge gained from this work provides a new aspect for further research towards genetic engineering of flavonoid biosynthesis in banana fruits to increase their antioxidant activity and nutritional value.

Introduction

Banana (*Musa* spp.) plants are well-known for their edible fruit and serve as a staple food crop in Africa, Central and South America (Arias et al., 2003). With more than 112 million tons produced in 2016, bananas are among the most popular fruits in the world and provide many employment opportunities (FAO, 2019). Furthermore, banana fruits are rich in health promoting minerals and phytochemicals, including flavonoids, a class of plant specialised metabolites, which contribute to the beneficial effects through their antioxidant characteristics (Forster et al., 2003; Wall, 2006; Singh et al., 2016). Flavonoid molecules share a C6-C3-C6 aglycon core, which can be reorganised or modified, e.g., by oxidation or glycosylation (Tanaka et al., 2008; Le Roy et al., 2016). Modifications at the central ring structure divide flavonoids into ten major subgroups (i.e. chalcones, aurones, flavanones, flavones, isoflavones, dihydroflavonols, flavonols, leucoanthocyanidins, anthocyanidins, and flavan-3-ols). The diversity in chemical structure is closely related to diverse bioactivities of flavonoids in plant biology and human nutrition (Falcone Ferreyra et al., 2012). For example, anthocyanins are in many cases well known to colour flowers and fruits to attract animals and thus promoting pollination and dispersion of seeds (Ishikura and Yoshitama, 1984; Gronquist et al., 2001; Grotewold, 2006). Flavonols can interact with anthocyanins to modify the colour of fruits

(Andersen and Jordheim, 2010) and play a prominent role in protection against UV-B irradiation (Li et al., 1993) and also in plant fertility (Mo et al., 1992).

Many researchers have attributed positive effects on human health to flavonoids: e.g., antigenotoxic (Dauer et al., 2003), anticarcinogenic and antioxidative (Kandil et al., 2002) effects, as well as the prevention of cardiovascular diseases have been suggested (summarised in Perez-Vizcaino and Duarte, 2010). Additionally, Sun et al. (2019) suggested an involvement of flavonoids in the plant defence against the tropical race 4 (TR4) of the *Musa* Fusarium wilt (commonly known as 'panama disease') pathogen *Fusarium oxysporum* f. sp. *cubense* (Foc), which is a threat to the global banana production. It is certainly interesting to take a closer look at the biosynthesis of flavonoids in *Musa*.

Flavonoids are derived from the amino acid L-phenylalanine and malonyl-coenzyme A. Their biosynthesis (Figure 1) has been analysed in many different species including the dicotyledonous model plant *Arabidopsis thaliana* (*A. thaliana*) (Hahlbrock and Scheel, 1989; Lepiniec et al., 2006) and the monocotyledonous crop plants *Zea mays* (*Z. mays*) (summarised in Tohge et al., 2017) and *Oryza sativa* (*O. sativa*) (summarised in Goufo and Trindade, 2014). The first committed step, catalysed by the enzyme chalcone synthase (CHS), is the formation of naringenin chalcone from *p*-coumaroyl CoA and malonyl CoA (Kreuzaler and Hahlbrock, 1972). A heterocyclic ring is introduced during the formation of naringenin (a flavanone) from naringenin chalcone, which can occur spontaneously or catalysed by chalcone isomerase (CHI) (Bednar and Hadcock, 1988). The enzyme flavanone 3-hydroxylase (F3H or FHT) converts flavanones to dihydroflavonols by hydroxylation at the C-3 position (Forkmann et al., 1980). Alternatively, flavanones can be converted to flavones by flavone synthase I or II (FNSI or II) (Britsch, 1990). Flavonol synthase (FLS) catalyses the conversion of dihydroflavonols to the corresponding flavonols by introducing a double bond between C-2 and C-3 (Forkmann et al., 1986; Holton et al., 1993). Moreover, dihydroflavonols can be converted to leucoanthocyanidins by dihydroflavonol 4-reductase (DFR) (Heller et al., 1985), which competes with FLS for substrates (Luo et al., 2016). Anthocyanidin synthase (ANS, also termed leucoanthocyanidin dioxygenase, LDOX) converts leucoanthocyanidins to anthocyanidins (Saito et al., 1999).

The flavonoid biosynthesis enzymes belong to different functional classes (summarised in Winkel, 2006): polyketide synthases (e.g., CHS), 2-oxoglutarate-dependent dioxygenases (2-ODD, e.g., F3H, ANS, FLS, FNSI), short-chain dehydrogenases/reductases (e.g., DFR), aldo-keto reductases (e.g., chalcone reductase, CHR) and cytochrome P450 monooxygenases (e.g., FNSII, F3′H). Flavonoid biosynthesis is evolutionary old in plants (Wen et al., 2020) and, although differences exist, quite similar in dicots like *A. thaliana* and monocots like *Musa* .

95 In the present study, we focus on the functional class of flavonoid aglycon forming enzymes,
96 namely the 2-ODDs. 2-ODDs occur throughout the kingdom of life and play important roles in
97 many biological processes including oxygen sensing and DNA repair (Jaakkola et al., 2001;
98 Trewick et al., 2002). They are a class of non-heme iron-containing enzymes, which require
99 2-oxoglutarate, Fe^{2+} and ascorbate for substrate conversion (summarised in Prescott and
100 John, 1996).
101 Plant 2-ODDs share conserved amino acid residues which coordinate ferrous iron binding
102 (HxDxnH) and binding of 2-oxoglutarate (RxS) (Cheng et al., 2014). They can be divided into
103 three distinct evolutionary classes, DOXA, DOXB and DOXC, based on amino acid similarity
104 (Kawai et al., 2014). The 2-ODDs involved in specialised metabolism were classified into the
105 DOXC class. Yet, all flavonoid biosynthesis related 2-ODDs were found in the DOXC
106 subclades 28 (F3H and FNSI) or 47 (FLS and ANS) (Kawai et al., 2014). In some cases, the
107 high amino acid similarity between the different enzymes leads to overlapping functions. For
108 example, FLSs from *Ginkgo biloba* (*G. biloba*) (Xu et al., 2012) and *O. sativa* (Park et al., 2019)
109 can accept flavanones and dihydroflavonols as substrates. Also, ANSs from *A. thaliana*
110 (Stracke et al., 2009) and *Malus domestica* (*M. domestica*) (Yan et al., 2005) can catalyse the
111 formation of flavonol glycosides.
112 Based on the *Musa acuminata* (*M. acuminata*) genome sequence annotation (DHont et al.,
113 2012), Pandey et al. (2016) identified 28 putative *Musa* flavonoid biosynthesis enzymes. This
114 includes seven 2-ODD-type enzymes, namely two F3H, four FLS and one ANS, while no
115 suitable FNSI candidate was identified. While the expression of the respective genes and
116 correlations of expression to flavonoid metabolite accumulation have been studied, the
117 functionality of these enzymes has not been analysed until now.
118 Here, we describe the sequence-based and functional characterisation of 2-ODDs from the
119 non-grass monocot *Musa*. Functionalities of recombinant *Musa* enzymes were analysed using
120 *in vivo* bioconversion assays and by *in planta* complementation of corresponding *A. thaliana*
121 loss-of-function mutants. This resulted in the experimental confirmation that the *Musa* flavonoid
122 2-ODDs studied have the predicted functions. The presented results contribute to the
123 understanding of flavonoid biosynthesis in *Musa*. They provide a strong basis for further
124 research to enhance the efficiency of flavonoid production in banana, in order to increase the
125 fruits' health promoting effects.
126
127
128 **Materials and Methods**
129
130 **Plant material**

131 Banana plants (Grand Naine, plantain) for RNA extraction were grown in the field in Lucknow,
132 India. *Musa* gene annotation identifiers refer to the study of Martin et al. (2016). Columbia-0
133 (Col-0, NASC ID N1092) and Nössen-0 (Nö-0, NASC ID N3081) were used as wildtype
134 controls. The *A. thaliana* mutants *tt6-2* (*f3h*, GK-292E08, Col-0 background) (Appelhagen et
135 al., 2014) and *ans/fls1-2* (synonym *ldox/fls1-2, ldox: SALK_028793,* Col-0 background; *fls1-2:*
136 RIKEN_PST16145, Nö-0 background) (Stracke et al., 2009) were used for complementation
137 experiments.
138
139 **Phylogenetic analysis**
140 Multiple protein sequence alignments were created with MAFFT v7 (Katoh and Standley, 2013)
141 using default settings. The Approximately-Maximum-Likelihood phylogenetic tree of 33 plant
142 2-ODDs with proven F3H, FNSI, FLS and ANS functionality (Supplementary Table S1) and
143 seven *Musa* 2-ODDs was constructed as described by Pucker et al. (2020b): MAFFT
144 alignments were cleaned with pxclsq (Brown et al., 2017) and the tree was constructed with
145 FastTree v2.1.10 using the WAG+CAT model (Price et al., 2010). The tree was visualised with
146 Interactive Tree Of Life (Letunic and Bork, 2019), branch lengths were neglected.
147
148 **Expression analysis**
149 Expression data for *Musa* 2-ODD genes was extracted from previous analyses (Pucker et al.,
150 2020a). Short Read Archive IDs can be found in Supplementary Table S2.
151
152 **Total RNA extraction, cDNA synthesis and molecular cloning**
153 Isolation of RNA from different *Musa* plant organs (leaf, pseudostem, bract, fruit peel, fruit pulp)
154 was performed according to a protocol from Asif et al. (2000). cDNA synthesis was performed
155 from 1 µg total RNA using the ProtoScript® First Strand cDNA Synthesis Kit (New England
156 Biolabs, NEB) with the provided random primer mix according to the suppliers' instructions.
157 Amplification of predicted full length CDSs (Pandey et al., 2016) were done using Q5® High-
158 Fidelity DNA polymerase (NEB) and gene-specific primers (Supplementary Table S3)
159 according to standard protocols. Creation of full-length coding sequence constructs (CDS) was
160 performed using the GATEWAY® Technology (Invitrogen). *MusaF3H1* (Ma02_t04650),
161 *MusaF3H2* (Ma07_t17200), *MusaFLS1* (Ma03_t06970), *MusaFLS3* (Ma10_t25110) and
162 *MusaANS* (Ma05_t03850) CDSs were successfully amplified on different cDNA pools. The
163 resulting PCR products were recombined into pDONR™/Zeo (Invitrogen) with BP clonase
164 (Invitrogen) resulting in Entry plasmids, which were sequenced by Sanger technology (Sanger
165 et al., 1977) on 3730XL sequencers using BigDye terminator v3.1 chemistry (Thermo Fisher).
166 Entry plasmids for *AtF3H*, *AtFLS1* and *AtMYB12* were available from previous studies (Preuss
167 et al., 2009; Stracke et al., 2017), *PcFNSI* was amplified on a plasmid from a previous study

168 (Martens et al., 2003). The full-length CDSs were introduced from the Entry plasmids into the
169 inducible *E. coli* expression vector pDEST17 (Invitrogen) and the binary expression vector
170 pLEELA (Jakoby et al., 2004) using GATEWAY LR-reaction (Invitrogen).
171
172 **Heterologous expression in *E. coli***
173 pDEST17-based plasmids containing *proT7*-RBS-6xHis-CDS-*T7term* expression cassettes
174 (*proT7: T7 promoter*, RBS: ribosome binding site, 6xHis: polyhistidine tag, *T7term: T7*
175 *transcription terminator*) were transformed into BL21-AI cells (Invitrogen). Cultures were grown
176 in LB to an OD_{600} of about 0.4 and expression was induced with 0.2 % L-arabinose.
177
178 **F3H and FLS bioconversion assay in *E. coli***
179 The enzyme assay was performed using 20 mL *E. coli* cultures expressing the respective
180 constructs right after induction with L-arabinose. 100 µL substrate (10 mg/mL naringenin,
181 eriodictyol or dihydroquercetin), 50 µL 2-oxoglutaric acid, 50 µL $FeSo_4$ and 50 µL 1 M sodium
182 ascorbate were added. The cultures were incubated at 28 °C overnight. To extract flavonoids,
183 1 mL was removed from each culture and mixed with 200 µL ethyl acetate by vortexing for
184 30 s. After centrifugation for 2 min. at 14,000 g, the organic phase was transferred into a fresh
185 reaction tube. Samples were taken after 0 h, 1 h, 2 h, 3 h, 4 h and 24 h. Flavonoid content was
186 analysed by high-performance thin-layer chromatography (HPTLC). Naringenin (Sigma),
187 dihydrokaempferol (Sigma), kaempferol (Roth), eriodictyol (TransMIT PlantMetaChem),
188 apigenin (TransMIT PlantMetaChem), dihydroquercetin (Roth) and quercetin (Sigma) were
189 dissolved in methanol and used as standards. 3 µL of each methanolic extract were spotted
190 on a HPTLC Silica Gel 60 plate (Merck). The mobile phase was composed of 50 % chloroform,
191 45 % acetic acid and 5 % water. Flavonoid compounds were detected as described previously
192 (Stracke et al., 2007), using diphenylboric acid 2-aminoethyl ester (DPBA) and UV-light
193 (Sheahan and Rechnitz, 1992).
194
195 ***Agrobacterium*-mediated transformation of *A. thaliana***
196 T-DNA from pLEELA-based plasmids containing *2xpro35S*-driven *Musa2-ODDs*, were
197 transformed into *A. thaliana* plants via *Agrobacterium tumefaciens* (Agrobacterium,
198 GV101::pMP90RK, (Koncz and Schell, 1986)) mediated gene transfer using the floral dip
199 method (Clough and Bent, 1998). Successful T-DNA integration was verified by BASTA
200 selection and PCR-based genotyping.
201
202 **Flavonoid staining of *A. thaliana* seedlings**
203 *In situ* visualisation of flavonoids in norflurazon-bleached *A. thaliana* seedlings was performed
204 according to Stracke et al. (2007) using DPBA/Triton X-100 and epifuorescence microscopy.

205

206 **Analysis of flavonols in methanolic extracts**

207 Flavonol glycosides were extracted and analysed as previously described (Stracke et al.,
208 2009). *A. thaliana* rosette leaves were homogenised in 80 % methanol, incubated for 15 min.
209 at 70 °C and centrifuged for 10 min. at 14,000 g. Supernatants were vacuum-dried. The dried
210 pellets were dissolved in 80 % methanol and analysed by HPTLC on a Silica Gel 60 plate
211 (Merck). Ethyl acetate, formic acid, acetic acid, water (100:26:12:12) were used as a mobile
212 phase. Flavonoid compounds were detected as described above.

213

214 **Determination of anthocyanin content**

215 To induce anthocyanin production, *A. thaliana* seedlings were grown on 0.5 MS plates with
216 4 % sucrose and 16 h of light illumination per day at 22 °C. Six day old seedlings were used
217 to photometrically quantify anthocyanins as described by Mehrtens et al. (2005). All samples
218 were measured in three independent biological replicates. Error bars indicate the standard
219 error of the average anthocyanin content. Statistical analysis was performed using the Mann–
220 Whitney U test (Mann and Whitney, 1947).

221

222

223 **Results**

224 **Creation of cDNA constructs and sequence based characterisation of *Musa* flavonoid**
225 **2-ODDs**

226 Previously described putative *Musa* flavonoid biosynthesis enzymes encoded in the
227 *M. acuminata* Pahang DH reference genome sequence were used. This included two F3Hs,
228 four FLSs and one ANS, which were classified as 2-ODDs. To functionally characterise these
229 *Musa* enzymes, we amplified the corresponding CDSs from a cDNA template collection
230 derived from different *Musa* organs, using primers designed on the Pahang DH reference
231 genome sequence. The successfully amplified cDNAs of *MusaF3H1* and *MusaF3H2* were
232 derived from plantain pulp, *MusaFLS1* from Grand Naine young leaf, *MusaFLS3* on Grand
233 Naine bract, and *MusaANS* on Grand Naine peel. Unfortunately, we were not able to amplify
234 *MusaFLS2* and *MusaFLS4* from our template collection.

235 Comparison of the resulting 2-ODD cDNA sequences with the reference sequence revealed
236 several single-nucleotide polymorphisms (SNPs) (Supplementary File S1). The derived amino
237 acid sequences show close similarity to other plant 2-ODD proteins known to be involved in
238 flavonoid biosynthesis (Supplementary File S2). The amino acids well known to coordinate
239 ferrous iron binding (HxDxnH) and binding of 2-oxoglutarate (RxS) are also conserved in the
240 *Musa* 2-ODDs. Additionally, the *At*FLS1 residues which have been shown to be involved in
241 flavonoid substrate binding (Supplementary File S2) are conserved. The residue F293 (all

242 positions refer to *At*FLS1) is conserved in all *Musa* 2-ODD proteins, F134 and K202 are found
243 in the *Musa*FLSs and *Musa*ANS and E295 is conserved in *Musa*ANS.
244 To analyse the evolutionary relationship between *Musa* 2-ODDs and 33 known flavonoid
245 biosynthesis related 2-ODDs, a phylogenetic tree was built (Figure 2). The phylogenetic tree
246 revealed two distinct clades, which correspond to the DOXC28 and DOXC47 classes of the
247 2-ODD superfamily. In the F3H and FNSI-containing DOXC28 class, *Musa*F3H1 and
248 *Musa*F3H2 cluster with other F3Hs from monocotyledonous plants. In the FLS and ANS-
249 containing DOXC47 class, the *Musa*ANS clusters with ANSs from monocotyledonous plants,
250 while the FLSs from monocotyledonous plants do not form a distinct group, although the
251 *Mus*aFLSs are in proximity to *Zm*FLS and *Os*FLS.
252 Our analyses clearly show that the CDSs identified for *Musa*F3H1, *Musa*F3H2, *Musa*FLS1,
253 *Musa*FLS3 and *Musa*ANS have the potential to encode functional flavonoid 2-ODDs.
254
255 **Expression profiles of *Musa 2-ODD* genes**
256 Analysis of the expression patterns of the genes studied was performed using published
257 RNA-Seq data. We obtained normalised RNA-Seq read values for *Musa* 2-ODD genes from
258 several organs and developmental stages (Table 1). *MusaF3H1* and *MusaF3H2* are
259 expressed in almost all analysed organs and developmental stages. *MusaF3H1* expression is
260 highest in early developmental stages of pulp (S1, S2), followed by intermediate
261 developmental stages of peel (S2, S3). *MusaF3H2* shows highest expression in adult leaves.
262 *MusaFLS2* was not expressed in any of the analysed samples. All four *MusaFLS* genes show
263 low or no expression in seedlings and embryonic cell suspension. *MusaFLS1* shows variance
264 in transcript abundance with particularly high levels in peel (S2) and in young and adult leaves.
265 *MusaFLS3* and *MusaFLS4* transcript levels are comparatively constant and low, with highest
266 transcript abundance in root and peel (S1 and S3 respectively). While *MusaFLS1* transcript
267 abundance is highest in adult leaf, *MusaFLS3* and *MusaFLS4* lack expression in this tissue.
268 *MusaANS* shows highest transcript abundance in pulp (S1, S2, S4) and peel (S3) and very
269 low expression in embryogenic cell suspension, seedlings and leaves.
270
271 ***Musa*F3H1 and *Musa*F3H2 are functional flavanone 3-hydroxylases**
272 To confirm F3H activity *in vivo*, we used a bioconversion assay. *MusaF3H1* and *MusaF3H2*
273 were heterologously expressed in *E. coli* and the bacterial cultures were fed with naringenin
274 or eriodictyol as substrate of F3H. Both recombinant proteins, *Musa*F3H1 and *Musa*F3H2,
275 were able to convert naringenin to dihydrokaempferol (DHK) in the presence of 2-oxoglutarate
276 and ferrous iron (Figure 3A). After 24 h of incubation, only small amounts of naringenin
277 remained un-converted. Conversion of the formed DHK to kaempferol by *Musa*F3H1 or
278 *Musa*F3H2 was not observed. Furthermore, eriodictyol was converted to dihydroquercetin

279 (DHQ) by *Musa*F3H1 and *Musa*F3H2 (Supplementary File S3). A further conversion to the
280 quercetin was not observed. Since *Musa*F3H2 was previously considered as FNSI candidate,
281 we analysed FNSI activity in a bioconversion assay. While *Musa*F3H2 was able to convert
282 naringenin to DHK we were not able to detect apigenin product in our approach
283 (Supplementary File S4). Accordingly, *Musa*F3H2 does not show FNSI activity in our assay.
284 For further *in planta* analysis we chose a complementation assay with an *A. thaliana f3h*
285 mutant *(tt6-2)* which expresses *FLS* and *ANS* but no *F3H*. *MusaF3H1* or *MusaF3H2* were
286 expressed in *tt6-2* plants under the control of the constitutive 2x35S promoter. The
287 accumulation of flavonol glycosides was analysed in herbizide-bleached seedlings using
288 DPBA-staining (Figure 3B). While Col-0 wildtype seedlings appeared yellow under UV light,
289 indicating the accumulation of flavonol glycosides, *tt6-2* seedlings showed a red fluorescence.
290 *tt6-2* mutants expressing *MusaF3H1* or *MusaF3H2* were able to complement the mutant
291 phenotype, showing the characteristic yellow flavonol glycoside fluorescence of the wild type.
292 These results demonstrate that *Musa*F3H1 and *Musa*F3H2 are functional enzymes with F3H
293 activity and are able to catalyse the conversion of naringenin to DHK.
294
295 ***Musa*FLS1 and *Musa*FLS3 are functional flavonol synthases**
296 To confirm FLS activity *in vivo*, the enzymes were assayed in a coupled bioconversion
297 experiment (Figure 4A). Two *E. coli* cultures expressing *MusaF3H1* and a *MusaFLS* were
298 mixed and fed with naringenin in the presence of 2-oxoglutarate and ferrous irons. Here,
299 *Musa*F3H1 converts naringenin to DHK, thus providing the substrate for the FLS enzyme to
300 be tested. While *Musa*FLS1 was found to be able to convert DHK to kaempferol under the
301 assay conditions, *Musa*FLS3 was not. In a second bioconversion experiment, *E. coli* cultures
302 expressing *MusaFLS1* or *MusaFLS3* were fed with DHQ (Supplementary File S5). Again,
303 *Musa*FLS1 was able convert the dihydroflavonol to the corresponding flavonol, while
304 *Musa*FLS3 was not. We checked the expression of recombinant *Musa*FLS1 and *Musa*FLS3 in
305 the *E. coli* cultures by SDS-PAGE and found both *Musa*FLS proteins being expressed at
306 similar levels (Supplementary File S7). Moreover, we analysed a possible F3H/FLS
307 biofunctional activity of *Musa*FLS1 and *Musa*FLS3 by feeding naringenin to *E. coli* cultures.
308 While *Musa*FLS1 was not able to convert naringenin to DHK in the assay, *Musa*FLS3 showed
309 F3H activity but not a further conversion to kaempferol (Supplementary File S6). To further
310 analyse the enzymatic properties *in planta*, *MusaFLS1* or *MusaFLS3* were expressed in the
311 flavonol and anthocyanin deficient *A. thaliana ans/fls1-2* double mutant. HPTLC analyses of
312 methanolic extracts from rosette leaves from greenhouse-grown plants (Figure 4B) showed
313 that wildtype plants (Col-0, Nö-0) contained flavonol glycosides, including the prominent
314 derivatives kaempferol 3-O-rhamnoside-7-O-rhamnoside (K-3R-7R), kaempferol 3-O-
315 glucoside-7-O-rhamnoside (K-3G-7R) and kaempferol 3[-O-rhamnosyl-glucoside[-7-O-

316 rhamnoside (K-3[G-R]-7R). *ans/fls1-2* plants accumulated several dihydroflavonols but did not
317 show flavonol derivatives. *ans/fls1-2* mutants transformed with 2x35S::*MusaFLS1* or
318 2x35S::*MusaFLS3* constructs were able to form several flavonol derivatives. Nevertheless,
319 intensities and accumulation patterns of flavonol glycosides varied. We also analysed if
320 *MusaFLS1* and *MusaFLS3* are able to complement the anthocyanin-deficiency of the *ans/fls1-*
321 *2* double mutant. For this, seedlings were grown on 4 % sucrose to induce anthocyanin
322 accumulation. As shown in Figure 4C, 6-day-old Col-0 and Nö-0 seedlings were able to
323 accumulate red anthocyanin pigments, while *ans/fls1-2* transformed with *MusaFLS1* or
324 *MusaFLS3* did not show visible anthocyanins. These results confirm that *Musa*FLS1 and
325 *Musa*FLS3 are functional proteins with FLS activity and are enzymes able to catalyse the
326 conversion of dihydroflavonol to flavonol.
327
328 ***Musa*ANS is a functional anthocyanidin synthase**
329 We analysed *Musa*ANS functionality in a complementation assay with the *ans/fls1-2*
330 *A. thaliana* double mutant. To examine the ability of *MusaANS* to complement the *ans/fls1-2*
331 anthocyanin deficiency phenotype, seedlings were grown on anthocyanin-inducing media.
332 Anthocyanin accumulation was analysed visually and quantified photometrically (Figure 5A-B).
333 While wildtype seedlings showed red pigmentation, the *ans/fls1-2* seedlings did not. *ans/fls1-2*
334 seedlings expressing *MusaANS* showed accumulation of anthocyanins. The anthocyanin
335 content in the complemented seedlings was strongly increased compared to *ans/fls1-2*
336 knockout plants, indicating ANS activity. Furthermore, we analysed the ability of *MusaANS* to
337 complement the flavonol deficiency phenotype of *ans/fls1-2* plants. For this, methanolic
338 extracts of seedlings were analysed by HPTLC followed by DPBA-staining (Figure 5C). While
339 wildtype seedlings accumulated several kaempferol and quercetin glycosides, *ans/fls1-2*
340 mutants expressing *MusaANS* showed a flavonoid pattern identical to the *ans/fls1-2* mutant,
341 accumulating dihydroflavonol derivatives, but no flavonol derivatives. These results indicate
342 that *Musa*ANS is a functional enzyme with ANS activity and is able to catalyse the conversion
343 of leucoanthocyanidin to anthocyanidin.
344
345 **Discussion**
346 In this study, we isolated several cDNAs of *in silico* annotated 2-ODD-type flavonoid
347 biosynthesis enzyme coding genes from *Musa* and tested the *in vivo* functionality of the
348 encoded proteins in *E. coli* and *A. thaliana*.
349
350 ***Musa*F3H1 and *Musa*F3H2**
351 *In vivo E. coli* bioconversion assays revealed that *Musa*F3H1 and *Musa*F3H2 can covert
352 naringenin to DHK. Moreover, *MusaF3H1* and *MusaF3H2* are able to complement the loss-of-

353 function phenotype of *A. thaliana tt6-2* seedlings, showing *in planta* F3H-activity. Therefore,
354 we conclude that *Musa*F3H1 and *Musa*F3H2 are functional flavanone 3-hydroxylases.
355 Previous studies annotated *Ma02_g04650* (*MusaF3H1*) and *Ma07_g17200* (*MusaF3H2*) as
356 genes encoding flavanone 3-hydroxylases (Martin et al., 2016; Pandey et al., 2016; Pucker et
357 al., 2020b). However, the automatic approach developed by Pucker et al. (2020b) also
358 considered *Ma07_g17200* as a candidate to encode a FNSI enzyme. For a parsley F3H protein
359 it has been found that a replacement of three amino acids was sufficient to cause FNSI side
360 activity and seven amino acid exchanges almost lead to a complete change in enzyme activity
361 towards FNSI functionality (Gebhardt et al., 2007). These findings underline the particular high
362 similarity between FNSI and F3H. A closer inspection of the deduced peptide sequence of
363 *Ma07_g17200* gene revealed a lack of conservation of amino acid residues known to be
364 relevant for FNSI function (i.e. T106M, T115I, I116V, F131I, E195D, I200V, V215L, R216K).
365 Furthermore, *Ma07_g17200* did not show FNSI activity in our bioconversion assay. Together
366 with the confirmed F3H activity, this indicates that the classification of *Ma07_g17200* as a FNSI
367 encoding gene was inaccurate. Even though Ma07_p17200 is no functional FNSI, flavone
368 derivatives have been identified in *Musa* (Fu et al., 2018). In *Gerbera* and *Glycine max*, FNSII
369 is responsible for the formation of flavones (Martens and Forkmann, 1999; Fliegmann et al.,
370 2010). A candidate *Musa*FNSII, encoded by *Ma08_g26160*, has been identified (Pucker et al.,
371 2020b) and is probably responsible for the accumulation of flavones in *Musa*. Since FNSII
372 enzymes are NADPH-dependent cytochrome P450 monooxygenases (Jiang et al., 2016), the
373 putative *Musa*FNSII (encoded by *Ma08_g26160*) was not studied in this work.
374 Our expression study that was based on published RNA-Seq data (Pucker et al., 2020a),
375 revealed highest *MusaF3H1* transcript abundance in early developmental stages of pulp and
376 intermediate stages of peel development, while highest *MusaF3H2* expression was found in
377 adult leaves (Table 1). This is, at first glance, in contrast to the quantitative real-time PCR
378 (qRT-PCR)-derived expression data presented by Pandey et al. (2016), reporting high
379 transcript levels of *MusaF3H1* and *MusaF3H2* in young leaves and bract. In this study, the
380 authors also show increased *MusaF3H1* expression in pseudostem, root and ripe pulp,
381 compared to *MusaF3H2*. These discrepancies are probably due to the different growth
382 conditions, germplasms/cultivars and sampling time points in the generation of the expression
383 data and cannot be reasonably analysed further at this point. It should be noted, however, that
384 *MusaF3H2* expression in leaves of plantlets was found to be increased following treatment
385 with the phytohormone methyl jasmonate (MJ), while *MusaF3H1* expression was not (Pandey
386 et al., 2016). As MJ is involved in various regulatory processes, including the response against
387 biotic and abiotic stresses (summarised in Cheong and Choi, 2003), the MJ-dependent
388 induction of *MusaF3H2* expression could imply that the *Musa*F3H2 enzyme plays a specialised
389 role in the formation of flavonoids in response to stresses. Such stress response induction of

390 F3H encoding genes was previously shown for a *F3H* gene from the dessert plant *Reaumuria*
391 *soongorica*, which is induced by UV-light (Liu et al., 2013) and two *F3H* genes from *Camellia*
392 *sinensis* (*C. sinensis*), which are induced by UV light and by treatment with abscisic acid (ABA)
393 or sucrose (Han et al., 2017). In addition, overexpression of *F3H* from *C. sinensis* (Mahajan
394 and Yadav, 2014) and from *Lycium chinense* (Song et al., 2016) in tobacco improved the
395 tolerance to salt stress and fungal pathogens in the first case and to drought stress in the latter
396 case. In conclusion, our results clearly show that *Musa*F3H1 and *Musa*F3H2 are functional
397 flavanone 3-hydroxylases and that *Musa*F3H2 might play a role in stress response.
398
399 ***Musa*FLS1 and *Musa*FLS3**
400 *Musa*FLS1 was found to be able to convert DHK and DHQ to the corresponding flavonol in the
401 *E. coli* bioconversion assays. This ability was validated *in planta* by successful
402 complementation of the flavonol deficiency of *A. thaliana ans/fls1-2* double mutant seedlings,
403 while the anthocyanin deficiency phenotype was not restored. These observations could hint
404 to an exclusive FLS activity of *Musa*FLS1. FLS and DFR, the first enzymes of the flavonol and
405 anthocyanin branches of flavonoid biosynthesis, compete for dihydroflavonol substrates
406 (Figure 1). This is demonstrated by several *A. thaliana fls1* single mutants which accumulate
407 higher levels of anthocyanin pigments (Owens et al., 2008; Stracke et al., 2009). Falcone
408 Ferreyra et al. (2010) found that overexpression of *ZmFLS1* in an *A. thaliana fls1* mutant
409 decreases the accumulation of anthocyanins to wildtype level, again indicating that the
410 anthocyanin and flavonol branches of flavonoid biosynthesis can compete for dihydroflavonol
411 substrates in the same cell or tissue. Accordingly, the overlapping substrate usage of FLS and
412 ANS is difficult to analyse in a *fls1* single mutant. Here, the use of an *A. thaliana ans/fls1-2*
413 double mutant is a simple way to analyse the FLS and a possible ANS side activity of flavonol
414 synthases and vice versa *in planta*. To analyse further side activities, a *f3h fls ans* mutant
415 would be beneficial. *A. thaliana ans/fls1-2* plants expressing *MusaFLS3* showed the
416 accumulation of several kaempferol derivatives. In contrast, plants complemented with
417 *MusaFLS1* also accumulate quercetin derivatives. This is most likely an effect of different
418 environmental conditions in plant growth. One set of plants was grown in the greenhouse
419 (*MusaFLS1*), another set was grown in a growth chamber (*MusaFLS3*). In the plants used for
420 *Musa*FLS3 experiments these conditions promoted the accumulation of DHQ, while the other
421 growth conditions did not in the plants used for *MusaFLS1* experiments. Accordingly, DHQ
422 was probably not available as a substrate for *Musa*FLS1 and could not be converted to
423 quercetin. A possible explanation for the varying DHQ amounts could be the light induced
424 expression of F3'H, which converts DHK to DHQ. The expression of *F3'H* in cultured *A.*
425 *thaliana* cells can be induced by UV-light (Schoenbohm et al., 2000) and the activity of the
426 *F3'H* promoter from *Vitis vinifera* is increased under light exposure (Sun et al., 2015).

427 Consequently, a different light quality or higher light intensity could be responsible for
428 increased *F3'H* expression, causing the accumulation of DHQ in the plants grown in the growth
429 chamber. While *MusaFLS3* was able to complement the flavonol deficiency in the *ans/fls1-2*
430 mutant, it did not lead to an accumulation of anthocyanins. In contrast to the *in planta* results,
431 *Musa*FLS3 did not convert DHK or DHQ to the corresponding flavonol in the *in vivo*
432 bioconversion assays, even though the protein was successfully expressed in the *E. coli*
433 culture. We used the bioconversion assays as a simple and versatile tool to analyse enzymatic
434 activities. Nevertheless, heterologous expression of eucaryotic proteins in *E. coli* is an artificial
435 system. It can cause a divergent pattern of posttranslational modifications or production of high
436 amounts of protein in inclusion bodies, leading to inactive protein (Sahdev et al., 2008). Preuss
437 et al. (2009) reported that *At*FLS3 did not show FLS activity in *E. coli*, but did convert
438 dihydroflavonols to the corresponding flavonols upon expression in yeast, indicating that the
439 stability of *At*FLS3 was improved under the latter assay conditions. The approach carried out
440 in this work might have similar limitations. Further limitations can be caused by different
441 substrate preferences, as reported for *Os*FLS (Park et al., 2019). Despite the lack of FLS
442 activity in the bioconversion assay, *Musa*FLS3 showed F3H activity. Nevertheless, the *in*
443 *planta* complementation of the flavonol deficiency in the *A. thaliana ans/fls1-2* mutant and the
444 lacking complementation of the anthocyanin deficiency phenotype in the *ans/fls1-2* mutant
445 indicate that *Musa*FLS3 is a functional flavonol synthase with F3H side activity, which does
446 not exhibit significant ANS activity.
447 *MusaFLS1* transcript abundance was found to be high in adult leaves and low in roots.
448 *MusaFLS3* and *MusaFLS4* revealed opposed transcript levels. Such divergent expression
449 patterns have previously been observed for *FLS1* and *FLS2* from *Freesia hybrida* and *FLS1*
450 and *FLS2* from *Cyclamen purpurascens* (Akita et al., 2018; Shan et al., 2020). These opposed
451 expression patterns could point to differential activity in distinct organs. Furthermore, the
452 tandemly arranged *MusaFLS3* and *MusaFLS4* genes show very similar expression patterns
453 (Table 1), possibly indicating functional redundancy. While we could not find expression of
454 *MusaFLS2* in our expression analyses, Pandey et al. (2016) observed *MusaFLS2* expression
455 in several organs (including bract, pseudostem and root), as well as in different developmental
456 stages of peel and pulp. Again, these results show that different cultivars, growth conditions,
457 sampling time points and analysed organs can have a strong influence on the resulting data.
458 Accordingly, data from different studies should be evaluated carefully. *MusaFLS1* and
459 *MusaFLS2* expression in leaves of plantlets does not significantly increase after MJ treatment
460 (Pandey et al., 2016). However, UV radiation induces the expression of FLS from *Z. mays*
461 (Falcone Ferreyra et al., 2010) and *M. domestica* (Henry-Kirk et al., 2018) and the relative
462 expression of FLS from *Triticum aestivum* increases during drought stress (Ma et al., 2014).
463 Together with the knowledge that flavonols act as antioxidants (Wang et al., 2006), an

464 involvement of *Musa*FLSs in stress response seems feasible and should be further analysed
465 under a broader range of conditions. In summary, our results show that *Musa*FLS1 and
466 *Musa*FLS3 are functional flavonol synthase enzymes and hint at possible differential organ
467 specific activities of *Musa*FLS1 and *Musa*FLS3 / *Musa*FLS4.
468
469 ***Musa*ANS**
470 *A. thaliana ans/fls1-2* seedlings expressing *MusaANS* show a strong, red pigmentation,
471 revealing that *MusaANS* can complement the anthocyanin deficiency caused by mutation of
472 *AtANS*. However, the seedlings did not display flavonol derivatives in HPTLC analyses, which
473 have been reported to detect flavonol glycosides at levels of 50 pMol (Stracke, 2010). These
474 results indicate that *Musa*ANS is a functional anthocyanidin synthase, but does not have FLS
475 activity. The RNA-Seq data-derived expression profiles revealed high *MusaANS* transcript
476 abundance in pulp and peel. Additionally, *MusaANS* expression has been reported to be high
477 in bract tissue (Pandey et al., 2016), the specialised leaves surrounding the flowers and usually
478 coloured red or purple due to anthocyanin accumulation (Pazmiño-Durána et al., 2001). This
479 spatial correlation of *MusaANS* transcripts and anthocyanin metabolites in bract tissue
480 supports the proposed biological functionality of this enzyme, catalysing the conversion of
481 leucoanthocyanidins to anthocyanidins in *Musa*. *MusaANS* expression increases 24 hours
482 after MJ treatment and decreases following dark treatment (Pandey et al., 2016). As supposed
483 for *MusaF3H2*, the increased expression of *MusaANS* after MJ treatment could imply an
484 involvement in the formation of anthocyanins as a consequence of stress response. ABA,
485 salicylic acid (SA), UV-B and cold treatments have been shown to enhance *ANS* transcript
486 abundance in *G. biloba* (Xu et al., 2008) and overexpression of *OsANS* raises the antioxidant
487 potential in *O. sativa* (Reddy et al., 2007). The accumulation of anthocyanins has often been
488 shown to be induced by (UV-) light (Takahashi et al., 1991; Stapleton and Walbot, 1994; Meng
489 et al., 2004). We therefore assume that also *Musa*ANS could be involved in such stress
490 response.
491 Very recently, a R2R3-MYB-type transcription factor (MaMYB4) has been identified as a
492 negative regulator of anthocyanin biosynthesis in *Musa* acting as repressor on the *MusaANS*
493 promoter (Deng et al., 2021). These results give a first insight into the transcriptional regulation
494 of *MusaANS* expression and confirm the role of *MusaANS* in the anthocyanin biosynthesis in
495 *Musa*. Taking all available evidence into account, *MusaANS* encodes a functional
496 anthocyanidin synthase with a possible involvement in the plants' stress response.
497
498 To deepen the knowledge about 2-ODDs and other enzymes involved in *Musa* flavonoid
499 biosynthesis, it would be beneficial to acquire even more spatially and timely highly resolved
500 transcriptome and in particular metabolite data. This data could serve as a starting point for

501 the analysis of organ-, stress- or development-specific enzyme activities and functions, as well
502 as possible substrate preferences. It could also be used to elucidate the regulatory network of
503 *Musa* flavonoid biosynthesis. Furthermore, knowledge about the influence of different stresses
504 (e.g., pathogens, light, temperature) on specific transcriptomes and metabolomes of the *Musa*
505 plant could help to widen the knowledge of flavonoid biosynthesis and particular the
506 functionality of the *Musa* 2-ODD enzymes. This could also lead to the detection of possible
507 restricted side activities or overlapping functionalities as described for 2-OODs in some other
508 plant species (Falcone Ferreyra et al., 2010; Park et al., 2019) and to further decode the cause
509 of these multifunctionalities in 2-ODDs.
510
511 To conclude, in this study the functionality of five 2-ODDs involved in flavonoid biosynthesis in
512 *Musa* was demonstrated *in vivo* in bacterial cells and *in planta*. Knowledge gained about the
513 structural genes *MusaF3H1*, *MusaF3H2*, *MusaFLS1*, *MusaFLS3* and *MusaANS* in a major
514 crop plant provides a basis for further research towards engineered, increased flavonoid
515 production in banana, which could contribute to the fruits' antioxidant activity and nutritional
516 value, and possibly even enhance the plants' defence against *Foc*-TR4.
517
518
519 **Conflict of Interest**
520 The authors declare that there is no conflict of interest.
521
522 **Author Contributions**
523 MB and RS planned the experiments. MB and CA performed the experiments and analysed
524 the data. MB and SM interpreted the TLC data. RS and BW supervised the project. MB wrote
525 the initial draft. RS and BW revised the manuscript. All authors read and approved the final
526 manuscript version.
527
528 **Funding**
529 This work was supported by basic funding of the chair of Genetics and Genomics of Plants
530 provided by Bielefeld University/Faculty of Biology.
531
532 **Acknowledgements**
533 We are grateful to Melanie Kuhlmann for her excellent assistance in the laboratory and to
534 Andrea Voigt for her competent help in the greenhouse. We thank Anika Beckers who
535 contributed to creation of constructs with *MusaFLS* cDNAs and Prisca Viehöver for
536 sequencing. In addition, we thank Thomas Baier for his support with the SDS-PAGE.
537

538 **Tables**

539

540 **Table 1: Expression profiles of *Musa2*-ODD genes in different organs and**
541 **developmental stages based on RNA-Seq data.** Expression levels are given in fragments
542 per kilo base per million mapped reads (FPKM). Different grey scales indicate expression
543 levels with higher levels given in darker grey. S1-S4 indicate stages of pulp and peel
544 developments from immature to ripe (Lu et al., 2018).

545

				leaf				pulp					peel				
gene	embryogenic	seedling	root	leaf	young leaf	adult leaf	old leaf	pulp	pulp S1	pulp S2	pulp S3	pulp S4	peel	peel S1	peel S2	peel S3	peel S4
MusaF3H1	3	9	80	44	73	27	3	170	385	191	43	60	82	46	140	104	36
MusaF3H2	21	0	23	57	39	171	7	32	96	14	3	14	19	7	27	33	9
MusaFLS1	6	0	4	189	91	643	16	2	2	1	2	2	29	3	99	7	7
MusaFLS2	0	0	0	0	0	0	0	0	0	0	0	0	0	0	0	0	0
MusaFLS3	0	0	32	16	17	0	0	16	15	22	10	17	22	27	16	20	25
MusaFLS4	0	0	19	4	0	0	0	10	11	4	12	13	15	16	11	19	14
MusaANS	1	3	90	41	79	3	1	255	559	298	26	137	73	47	50	163	30

546

547

548 **Figure legends**

549

550 **Figure 1: Schematic, simplified illustration of the core flavonoid aglycon biosynthesis**
551 **pathway in plants.**
552 Chalcone synthase (CHS), the first committed enzyme in flavonoid biosynthesis, connects a
553 CoA ester and malonyl-CoA, forming a chalcone. Chalcone isomerase (CHI) introduces the
554 heterocyclic ring. The resulting flavanone is converted to dihydroflavonol by flavanone 3-
555 hydroxylase (F3H) or to flavones by flavone synthase (FNSI or FNSII). Dihydroflavonols are
556 converted to flavonols by flavonol synthase (FLS). Alternatively, dihydroflavonol 4-reductase
557 (DFR) can reduce dihydroflavonols to the corresponding leucoanthocyanidin, which is
558 converted to anthocyanidin by the activity of anthocyanidin synthase (ANS). Flavonoid 3'
559 hydroxylase (F3‘H) hydroxylates 3‘ position of the B-ring using different flavonoid substrates.
560 2-oxoglutarate-dependant oxygenases are given in bold underlined. Enzymes in the focus of
561 this work are highlighted by grey boxes.

562

563 **Figure 2: Rooted Approximately-Maximum-Likelihood (ML) phylogenetic tree of 2-ODDs**
564 **involved in flavonoid biosynthesis.**
565 ODDs from Banana are given in blue, 39 enzymes with proven F3H, FNSI, FLS or ANS activity
566 were included. Different grey scales indicate F3H, FLS, ANS and two evolutionary FNSI
567 clades. *At*GA3ox1 (gibberellin 3 beta-hydroxylase1) was used as an outgroup. Branchpoints
568 to DOXC28 and DOXC47 classes are marked with black arrowheads.
569
570 **Figure 3: *Musa*F3H1 and *Musa*F3H2 are functional flavanone 3-hydroxylases.**
571 (A) HPTLC analysis of F3H bioconversion assays using extracts from *E. coli* expressing
572 recombinant *Musa*F3H1 or *Musa*F3H2. The substrate naringenin (N) and the product
573 dihydrokaempferol (DHK) were used as standards. *At*F3H was used as a positive control.
574 *At*MYB12 was used as a negative control. (B) Analysis of *tt6-2* mutant seedlings
575 complemented with *Musa*F3H1 and *Musa*F3H2. Col-0 wildtype and *tt6-2* were used as
576 controls. Representative pictures of DPBA-stained seedlings under UV light are given. Yellow
577 fluorescence indicates flavonol glycoside accumulation. The different numbers indicate
578 individual transgenic lines. The scale bar indicates 0.5 mm.
579
580
581 **Figure 4: *Musa*FLS1 and *Musa*FLS3 are functional flavonol synthases.**
582 (A) HPTLC analysis of a FLS bioconversion assays using extracts from *E. coli* expressing
583 recombinant *Musa*FLS1 or *Musa*FLS3. The F3H substrate naringenin (N), the FLS substrate
584 dihydrokaempferol (DHK) and the product kaempferol (K) were used as standards. *At*FLS1
585 served as a positive control and *At*MYB12 was used as a negative control. (B) Flavonol
586 glycoside accumulation in *Musa*FLS-complemented *ans/fls1-2* seedlings, analysed by HPTLC
587 analysis. Col-0, Nö-0 (both wildtype) and *ans/fls1-2* were used as controls. Bright green spots
588 belong to derivates of kaempferol, orange spots are derivates of quercetin and faint blue shows
589 sinapate derivatives. Dark green and yellow spots indicate DHK and DHQ, respectively. G,
590 glucose; K, kaempferol; Q, quercetin; R, rhamnose (C) Representative pictures of anthocyanin
591 (red) accumulation in 6-day-old *Musa*FLS-complemented *ans/fls1-2* seedlings growing on 4 %
592 sucrose. The scale bar indicates 0.5 mm.
593
594 **Figure 5: *Musa*ANS is a functional anthocyanin synthase.**
595 Analysis of *ans/fls1-2* double mutant seedlings complemented with 2x35S driven *MusaANS*
596 demonstrate *in planta* ANS functionality of *Musa*ANS by anthocyanin accumulation. The
597 different numbers indicate individual transgenic lines. (A-B) Sucrose induced anthocyanin
598 accumulation in 6-day-old *A. thaliana* seedlings. (A) Representative pictures of seedlings (the
599 scale bar indicates 0.5 mm) and (B) corresponding relative anthocyanin content. Error bars

600 indicate the standard error for three independent measurements. (C) *Musa*ANS does not show
601 *in planta* FLS activity. Flavonol glycoside accumulation in *MusaANS*-complemented *ans/fls1-*
602 *2* seedlings, analysed by HPTLC analysis. Col-0, Nö-0 (both wildtype) and *ans/fls1-2* were
603 used as controls. Bright green spots belong to derivates of kaempferol, orange spots are
604 derivates of quercetin and faint blue shows sinapate derivatives. Dark green and yellow spots
605 indicate DHK and DHQ, respectively. G, glucose; K, kaempferol; Q, quercetin; R, rhamnose.
606

607 **Supplementary Material**

608 Table S1: Plant 2-ODDs with proven F3H, FNSI, FLS and ANS functionality, used in
609 phylogenetic analysis.

610 Table S2: Sequence Read Archive IDs for RNA-Seq raw data used for expression analysis.

611 Table S3: Oligonucleotide primers, used in this work.

612 File S1: CDS of *Musa2*-ODDs from this work.

613 File S2: Multiple sequence alignment of flavonoid biosynthesis related 2-ODDs from banana
614 and plant proteins with demonstrated 2-ODD activity.

615 File S3: *Musa*F3H1 and *Musa*F3H2 convert eriodictyol to dihydroquercetin.

616 File S4: Analysis of FNSI side activity of *Musa*F3H2.

617 File S5: MusaFLS1 converts dihydroquercetin to quercetin.

618 File S6: Analysis of F3H side activity of *Musa*FLS1 and *Musa*FLS3.

619 File S7: Analysis of recombinant *Musa*FLS1 and *Musa*FLS3 in *E. coli* by SDS-PAGE.

620

621 **References**

622 Akita, Y., Kitamura, S., Mikami, R., and Ishizaka, H. (2018). Identification of functional
623 flavonol synthase genes from fragrant wild cyclamen (Cyclamen purpurascens).
624 *Journal of Plant Biochemistry and Biotechnology* 27(2), 147-155. doi:
625 https://doi.org/10.1007/s13562-017-0423-9.
626 Andersen, Ø.M., and Jordheim, M. (2010). "Anthocyanins," in *Encyclopedia of Life Sciences*.
627 (Chichester: John Wiley &Sons, Ltd).
628 Appelhagen, I., Thiedig, K., Nordholt, N., Schmidt, N., Huep, G., Sagasser, M., et al. (2014).
629 Update on *transparent testa* mutants from *Arabidopsis thaliana*: characterisation of
630 new alleles from an isogenic collection. *Planta* 240(5), 955-970.
631 Arias, P., Dankers, C., Liu, P., and Pilkauskas, P. (2003). The World Banana Economy,
632 1985-2002. http://www.fao.org/3/y5102e/y5102e5100.htm.

633 Asif, M.H., Dhawan, P., and Nath, P. (2000). A simple procedure for the isolation of high
634 quality RNA from ripening banana fruit. *Plant Molecular Biology Reporter* 18**,** 109-
635 115.
636 Bednar, R.A., and Hadcock, J.R. (1988). Purification and Characterizationo of Chalcone
637 Isomerase from Soybeans. *Journal of Biological Chemistry* 263**,** 9582-9588
638 Britsch, L. (1990). Purification and Characterization of Flavone Synthase I, a 2-Oxoglutarate-
639 Dependent Desaturase. *Archives of Biochemistry and Biophysics* 282(1)**,** 152-160.
640 Brown, J.W., Walker, J.F., and Smith, S.A. (2017). Phyx: phylogenetic tools for unix.
641 *Bioinformatics* 33(12)**,** 1886-1888. doi: 10.1093/bioinformatics/btx063.
642 Cheng, A.X., Han, X.J., Wu, Y.F., and Lou, H.X. (2014). The function and catalysis of 2-
643 oxoglutarate-dependent oxygenases involved in plant flavonoid biosynthesis.
644 *International Journal of Molecular Sciences* 15(1)**,** 1080-1095.
645 Cheong, J.-J., and Choi, Y.D. (2003). Methyl jasmonate as a vital substance in plants.
646 *Trends in Genetics* 19(7)**,** 409-413. doi: 10.1016/S0168-9525(03)00138-0.
647 Clough, S.J., and Bent, A.F. (1998). Floral dip: a simplified method for Agrobacterium-
648 mediated transformation of *Arabidopsis thaliana*. *The Plant Journal* 16(6)**,** 735-743.
649 doi: 10.1046/j.1365-313x.1998.00343.x.
650 Dauer, A., Hensel, A., Lhoste, E., Knasmüller, S., and Mersch-Sundermann, V. (2003).
651 Genotoxic and antigenotoxic effects of catechin and tannins from the bark of
652 Hamamelis virginiana L. in metabolically competent, human hepatoma cells (Hep G2)
653 using single cell gel electrophoresis. *Phytochemistry* 63(2)**,** 199-207. doi:
654 10.1016/S0031-9422(03)00104-3.
655 Deng, G.M., Zhang, S., Yang, Q.S., Gao, H.J., Sheng, O., Bi, F.C., et al. (2021). MaMYB4,
656 an R2R3-MYB Repressor Transcription Factor, Negatively Regulates the
657 Biosynthesis of Anthocyanin in Banana. *Frontiers in Plant Science* 11**,** 600704. doi:
658 10.3389/fpls.2020.600704.
659 DHont, A., Denoeud, F., Aury, J.M., Baurens, F.C., Carreel, F., Garsmeur, O., et al. (2012).
660 The banana (Musa acuminata) genome and the evolution of monocotyledonous
661 plants. *Nature* 488(7410)**,** 213-217.
662 Falcone Ferreyra, M.L., Rius, S., Emiliani, J., Pourcel, L., Feller, A., Morohashi, K., et al.
663 (2010). Cloning and characterization of a UV-B-inducible maize flavonol synthase.
664 *The Plant Journal* 62(1)**,** 77-91. doi: 10.1111/j.1365-313X.2010.04133.x.
665 Falcone Ferreyra, M.L., Rius, S.P., and Casati, P. (2012). Flavonoids: biosynthesis,
666 biological functions, and biotechnological applications. *Frontiers in Plant Science* 3**,**
667 222. doi: 10.3389/fpls.2012.00222.
668 FAO (2019). "The State of Food and Agriculture 2019". (Rome, Italy: Food and Agricultural
669 Organization (FAO)).
670 Fliegmann, J., Furtwangler, K., Malterer, G., Cantarello, C., Schuler, G., Ebel, J., et al.
671 (2010). Flavone synthase II (CYP93B16) from soybean (Glycine max L.).
672 *Phytochemistry* 71(5-6)**,** 508-514. doi: 10.1016/j.phytochem.2010.01.007.
673 Forkmann, G., de Vlaming, P., Spribille, R., Wiering, H., and Schram, W. (1986). Genetic and
674 Biochemical Studies on the Conversion of Dihydroflavonols to Flavonols in Flowers of
675 *Petunia hybrida*. *Zeitschrift für Naturforschung C* 41(1-2)**,** 179-186.
676 Forkmann, G., Heller, W., and Grisebach, H. (1980). Anthocyanin Biosynthesis in Flowers of
677 *Matthiola incana* Flavanone 3- and Flavonoid 3'-Hydroxylases. *Zeitschrift für*
678 *Naturforschung C* 35(9-10)**,** 691-695. doi: doi.org/10.1515/znc-1980-9-1004.
679 Forster, M., Rodríguez, E.R., Martín, J.D., and Romero, C.D. (2003). Distribution of Nutrients
680 in Edible Banana Pulp. *Food Technology and Biotechnology* 41(2)**,** 167-171.
681 Fu, X., Cheng, S., Liao, Y., Huang, B., Du, B., Zeng, W., et al. (2018). Comparative analysis
682 of pigments in red and yellow banana fruit. *Food Chemistry* 239**,** 1009-1018. doi:
683 10.1016/j.foodchem.2017.07.046.
684 Gebhardt, Y.H., Witte, S., Steuber, H., Matern, U., and Martens, S. (2007). Evolution of
685 flavone synthase I from parsley flavanone 3beta-hydroxylase by site-directed
686 mutagenesis. *Plant Physiology* 144(3)**,** 1442-1454. doi: doi: 10.1104/pp.18.00463.

687 Goufo, P., and Trindade, H. (2014). Rice antioxidants: phenolic acids, flavonoids,
688 anthocyanins, proanthocyanidins, tocopherols, tocotrienols, gamma-oryzanol, and
689 phytic acid. *Food Science & Nutrition* 2(2), 75-104. doi: 10.1002/fsn3.86.
690 Gronquist, M., Bezzerides, A., Attygalle, A., Meinwald, J., Eisner, M., and Eisner, T. (2001).
691 Attractive and defensive functions of the ultraviolet pigments of a flower *(Hypericum*
692 *calycinum)*. *Proceedings of the National Academie of Sciences of the United States*
693 *of America* 98(24), 13745-13750.
694 Grotewold, E. (2006). *The Science of Flavonoids.* Columbus: The Ohio State University.
695 Hahlbrock, K., and Scheel, D. (1989). Physiology and molecular biology of phenylpropanoid
696 metabolism. *Annual Review of Plant Physiology and Plant Molecular Biology* 40(1),
697 347-369. doi: 10.1146/annurev.pp.40.060189.002023.
698 Han, Y., Huang, K., Liu, Y., Jiao, T., Ma, G., Qian, Y., et al. (2017). Functional Analysis of
699 Two Flavanone-3-Hydroxylase Genes from *Camellia sinensis*: A Critical Role in
700 Flavonoid Accumulation. *Genes* 8(11). doi: 10.3390/genes8110300.
701 Heller, W., Forkmann, G., Britsch, L., and Grisebach, H. (1985). Enzymatic reduction of (+)-
702 dihydroflavonols to flavan-3,4-cis-diols with flower extracts from *Matthiola incana* and
703 its role in anthocyanin biosynthesis. *Planta* 165, 284-287.
704 Henry-Kirk, R.A., Plunkett, B., Hall, M., McGhie, T., Allan, A.C., Wargent, J.J., et al. (2018).
705 Solar UV light regulates flavonoid metabolism in apple (Malus x domestica). *Plant,*
706 *Cell & Environment* 41(3), 675-688. doi: 10.1111/pce.13125.
707 Holton, T.A., Brugliera, F., and Tanaka, Y. (1993). Cloning and expression of flavonol
708 synthase from *Petunia hybrida*. *The Plant Journal* 4, 1003-1010. doi: 10.1046/j.1365-
709 313x.1993.04061003.x.
710 Ishikura, N., and Yoshitama, K. (1984). Anthocyanin-Flavonol Co-pigmentation in Blue Seed
711 Coats of Ophiopogon jaburan. *Journal of Plant Physiology* 115(2), 171-175. doi:
712 10.1016/s0176-1617(84)80064-4.
713 Jaakkola, P., Mole, D.R., Tian, Y.M., Wilson, M.I., Gielbert, J., Gaskell, S.J., et al. (2001).
714 Targeting of HIF-alpha to the von Hippel-Lindau ubiquitylation complex by O2-
715 regulated prolyl hydroxylation. *Science* 292(5516), 468-472. doi:
716 10.1126/science.1059796.
717 Jakoby, M., Wang, H.Y., Reidt, W., Weisshaar, B., and Bauer, P. (2004). FRU (BHLH029) is
718 required for induction of iron mobilization genes in Arabidopsis thaliana. *FEBS Letters*
719 577(3), 528-534.
720 Jiang, N., Doseff, A.I., and Grotewold, E. (2016). Flavones: From Biosynthesis to Health
721 Benefits. *Plants* 5(2). doi: 10.3390/plants5020027.
722 Kandil, F.E., Smith, M.A., Rogers, R.B., Pepin, M.F., Song, L.L., Pezzuto, J.M., et al. (2002).
723 Composition of a chemopreventive proanthocyanidin-rich fraction from cranberry
724 fruits responsible for the inhibition of 12-O-tetradecanoyl phorbol-13-acetate (TPA)-
725 induced ornithine decarboxylase (ODC) activity. *Journal of Agricultural and Food*
726 *Chemistry* 50(5), 1063-1069. doi: 10.1021/jf011136z.
727 Katoh, K., and Standley, D.M. (2013). MAFFT multiple sequence alignment software version
728 7: improvements in performance and usability. *Molecular Biology and Evolution* 30(4),
729 772-780.
730 Kawai, Y., Ono, E., and Mizutani, M. (2014). Evolution and diversity of the 2-oxoglutarate-
731 dependent dioxygenase superfamily in plants. *The Plant Journal* 78(2), 328-343. doi:
732 10.1111/tpj.12479.
733 Koncz, C., and Schell, J. (1986). The promoter of TL-DNA gene 5 controls the tissue-specific
734 expression of chimaeric genes carried by a novel type of Agrobacterium binary
735 vector. *Molecular Genetics and Genomics* 204, 383-396.
736 Kreuzaler, F., and Hahlbrock, K. (1972). Enzymatic synthesis of aromatic compounds in
737 higher plants: formation of naringenin (5,7,4'-trihydroxyflavanone) from p-coumaroyl
738 coenzyme A and malonyl coenzyme A *FEBS Letters* 28(1), 69-72.
739 Le Roy, J., Huss, B., Creach, A., Hawkins, S., and Neutelings, G. (2016). Glycosylation Is a
740 Major Regulator of Phenylpropanoid Availability and Biological Activity in Plants.
741 *Frontiers in Plant Science* 7, 735.

742 Lepiniec, L., Debeaujon, I., Routaboul, J.M., Baudry, A., Pourcel, L., Nesi, N., et al. (2006).
743 Genetics and biochemistry of seed flavonoids. *Annual Review of Plant Biology* 57**,**
744 405-430.
745 Letunic, I., and Bork, P. (2019). Interactive Tree Of Life (iTOL) v4: recent updates and new
746 developments. *Nucleic Acids Research* 47(W1)**,** W256-W259. doi:
747 10.1093/nar/gkz239.
748 Li, J., Ou-Lee, T.M., Raba, R., Amundson, R.G., and Last, R.L. (1993). Arabidopsis
749 Flavonoid Mutants Are Hypersensitive to UV-B Irradiation. *The Plant Cell* 5(2)**,** 171-
750 179. doi: 10.1105/tpc.5.2.171.
751 Liu, M., Li, X., Liu, Y., and Cao, B. (2013). Regulation of flavanone 3-hydroxylase gene
752 involved in the flavonoid biosynthesis pathway in response to UV-B radiation and
753 drought stress in the desert plant, Reaumuria soongorica. *Plant Physiology and*
754 *Biochemistry* 73**,** 161-167. doi: 10.1016/j.plaphy.2013.09.016.
755 Lu, P., Yu, S., Zhu, N., Chen, Y.R., Zhou, B., Pan, Y., et al. (2018). Genome encode
756 analyses reveal the basis of convergent evolution of fleshy fruit ripening. *Nature*
757 *Plants* 4(10)**,** 784-791. doi: https://doi.org/10.1038/s41477-018-0249-z.
758 Luo, P., Ning, G., Wang, Z., Shen, Y., Jin, H., Li, P., et al. (2016). Disequilibrium of Flavonol
759 Synthase and Dihydroflavonol-4-Reductase Expression Associated Tightly to White
760 vs. Red Color Flower Formation in Plants. *Frontiers in Plant Science* 6**,** 1257. doi:
761 10.3389/fpls.2015.01257.
762 Ma, D.Y., Sun, D.X., Wang, C.Y., Li, Y.G., and Guo, T.C. (2014). Expression of flavonoid
763 biosynthesis genes and accumulation of flavonoid in wheat leaves in response to
764 drought stress. *Plant Physiology and Biochemistry* 80**,** 60-66. doi:
765 http://dx.doi.org/10.1016/j.plaphy.2014.03.024.
766 Mahajan, M., and Yadav, S.K. (2014). Overexpression of a tea flavanone 3-hydroxylase
767 gene confers tolerance to salt stress and Alternaria solani in transgenic tobacco.
768 *Plant Molecular Biology* 85(6)**,** 551-573. doi: 10.1007/s11103-014-0203-z.
769 Mann, H.B., and Whitney, D.R. (1947). On a Test of Whether One of Two Random Variables
770 Is Stochastically Larger than the Other. The Annals of Mathematical Statistics 18(1),
771 50-60. doi: 10.1214/aoms/1177730491.
772 Martens, S., and Forkmann, G. (1999). Cloning and expression of flavone synthase II from
773 Gerbera hybrids. *The Plant Journal* 20(5)**,** 611-618.
774 Martens, S., Forkmann, G., Britsch, L., Wellmann, F., Matern, U., and Lukacin, R. (2003).
775 Divergent evolution of flavonoid 2-oxoglutarate-dependent dioxygenases in parsley.
776 FEBS Letters 544(1-3), 93-98. doi: 10.1016/s0014-5793(03)00479-4.
777 Martin, G., Baurens, F.C., Droc, G., Rouard, M., Cenci, A., Kilian, A., et al. (2016).
778 Improvement of the banana "Musa acuminata" reference sequence using NGS data
779 and semi-automated bioinformatics methods. *BMC Genetics* 17(243).
780 Mehrtens, F., Kranz, H., Bednarek, P., and Weisshaar, B. (2005). The Arabidopsis
781 transcription factor MYB12 is a flavonol-specific regulator of phenylpropanoid
782 biosynthesis. *Plant Physiology* 138(2)**,** 1083-1096.
783 Meng, X., Xing, T., and Wang, X. (2004). The role of light in the regulation of anthocyanin
784 accumulation in Gerbera hybrida. *Plant Growth Regulation* 44(3)**,** 243-250. doi:
785 10.1007/s10725-004-4454-6.
786 Mo, Y., Nagel, C., and Taylor, L.P. (1992). Biochemical complementation of chalcone
787 synthase mutants defines a role for flavonols in functional pollen. *Proceedings of the*
788 *National Academy of Sciences of the United States of America* 89**,** 7213-7217.
789 Owens, D.K., Alerding, A.B., Crosby, K.C., Bandara, A.B., Westwood, J.H., and Winkel, B.S.
790 (2008). Functional analysis of a predicted flavonol synthase gene family in
791 Arabidopsis. *Plant Physiology* 147(3)**,** 1046-1061. doi: 10.1104/pp.108.117457.
792 Pandey, A., Alok, A., Lakhwani, D., Singh, J., Asif
793 , M.H., and Trivedi, P.K. (2016). Genome-wide Expression Analysis and Metabolite Profiling
794 Elucidate Transcriptional Regulation of Flavonoid Biosynthesis and Modulation under
795 Abiotic Stresses in Banana. *Scientific Reports* 6.
796 Park, S., Kim, D.H., Park, B.R., Lee, J.Y., and Lim, S.H. (2019). Molecular and Functional
797 Characterization of Oryza sativa Flavonol Synthase (OsFLS), a Bifunctional

Dioxygenase. *Journal of Agricultural and Food Chemistry* 67(26), 7399-7409. doi: 10.1021/acs.jafc.9b02142.

Pazmiño-Durána, E.A., Giustib, M.M., Wrolstad, R.E., and Glóriaa, M.B.A. (2001). Anthocyanins from banana bracts (Musa X paradisiaca) as potential food colorants. *Food Chemistry* 73, 327-332. doi: doi.org/10.1016/S0308-8146(00)00305-8.

Perez-Vizcaino, F., and Duarte, J. (2010). Flavonols and cardiovascular disease. *Molecular Aspects of Medicine* 31(6), 478-494. doi: 10.1016/j.mam.2010.09.002.

Prescott, A.G., and John, P. (1996). DIOXYGENASES: Molecular Structure and Role in Plant Metabolism. *Annual Review of Plant Physiology and Plant Molecular Biology* 47, 245-271. doi: doi.org/10.1146/annurev.arplant.47.1.245.

Preuss, A., Stracke, R., Weisshaar, B., Hillebrecht, A., Matern, U., and Martens, S. (2009). *Arabidopsis thaliana* expresses a second functional flavonol synthase. *FEBS Letters* 583(12), 1981–1986. doi: 10.1016/j.febslet.2009.05.006.

Price, M.N., Dehal, P.S., and Arkin, A.P. (2010). FastTree 2--approximately maximum-likelihood trees for large alignments. *PLoS One* 5(3), e9490. doi: 10.1371/journal.pone.0009490.

Pucker, B., Pandey, A., Weisshaar, B., and Stracke, R. (2020a). The R2R3-MYB gene family in banana (Musa acuminata): Genome-wide identification, classification and expression patterns. *PLoS One* 15(10), e0239275. doi: 10.1371/journal.pone.0239275.

Pucker, B., Reiher, F., and Schilbert, H.M. (2020b). Automatic Identification of Players in the Flavonoid Biosynthesis with Application on the Biomedicinal Plant Croton tiglium. *Plants* 9(9). doi: 10.3390/plants9091103.

Reddy, A.M., Reddy, V.S., Scheffler, B.E., Wienand, U., and Reddy, A.R. (2007). Novel transgenic rice overexpressing anthocyanidin synthase accumulates a mixture of flavonoids leading to an increased antioxidant potential. *Metabolic Engineering* 9(1), 95-111. doi: https://doi.org/10.1016/j.ymben.2006.09.003.

Sahdev, S., Khattar, S.K., and Saini, K.S. (2008). Production of active eukaryotic proteins through bacterial expression systems: a review of the existing biotechnology strategies. *Molecular and Cellular Biochemistry* 307(1-2), 249-264. doi: 10.1007/s11010-007-9603-6.

Saito, K., Kobayashi, M., Gong, Z.Z., Tanaka, Y., and Yamazaki, M. (1999). Direct evidence for anthocyanidin synthase as a 2-oxoglutarate-dependent oxygenase: molecular cloning and functional expression of cDNA from a red forma of Perilla frutescens. *The Plant Journal* 17(2), 181-189.

Sanger, F., Nicklen, S., and Coulson, A.R. (1977). DNA sequencing with chain-terminating inhibitors. *Proceedings of the National Academy of Sciences of the United States of America* 74(12), 5463-5467.

Schoenbohm, C., Martens, S., Eder, C., Forkmann, G., and Weisshaar, B. (2000). Identification of the *Arabidopsis thaliana* flavonoid 3'-hydroxylase gene and functional expression of the encoded P450 enzyme. *Biological Chemistry* 381, 749-753.

Shan, X., Li, Y., Yang, S., Yang, Z., Qiu, M., Gao, R., et al. (2020). The spatio-temporal biosynthesis of floral flavonols is controlled by differential phylogenetic MYB regulators in Freesia hybrida. *New Phytologist*. doi: 10.1111/nph.16818.

Sheahan, J.J., and Rechnitz, G.A. (1992). Flavonoid-specific staining of Arabidopsis thaliana. *BioTechniques* 13(6), 880-883.

Singh, B., Singh, J.P., Kaur, A., and Singh, N. (2016). Bioactive compounds in banana and their associated health benefits - A review. *Food Chemistry* 206, 1-11. doi: 10.1016/j.foodchem.2016.03.033.

Song, X., Diao, J., Ji, J., Wang, G., Guan, C., Jin, C., et al. (2016). Molecular cloning and identification of a flavanone 3-hydroxylase gene from *Lycium chinense*, and its overexpression enhances drought stress in tobacco. *Plant Physiol Biochem* 98, 89-100. doi: 10.1016/j.plaphy.2015.11.011.

Stapleton, A.E., and Walbot, V. (1994). Flavonoids can protect maize DNA from the induction of ultraviolet radiation damage. *Plant Physiology* 105, 881-889.

Stracke, R., De Vos, R.C.H., Bartelniewoehner, L., Ishihara, H., Sagasser, M., Martens, S., et al. (2009). Metabolomic and genetic analyses of flavonol synthesis in *Arabidopsis thaliana* support the *in vivo* involvement of leucoanthocyanidin dioxygenase. *Planta* 229(2)**,** 427-445. doi: 10.1007/s00425-008-0841-y.

Stracke, R., Ishihara, H., Huep, G., Barsch, A., Mehrtens, F., Niehaus, K., et al. (2007). Differential regulation of closely related R2R3-MYB transcription factors controls flavonol accumulation in different parts of the *Arabidopsis thaliana* seedling. *The Plant Journal* 50(4)**,** 660-677. doi: 10.1111/j.1365-313X.2007.03078.x.

Stracke, R., Turgut-Kara, N., and Weisshaar, B. (2017). The AtMYB12 activation domain maps to a short C-terminal region of the transcription factor. *Zeitschrift für Naturforschung C* 72(7-8)**,** 251-257. doi: 10.1515/znc-2016-0221.

Sun, J., Zhang, J., Fang, H., Peng, L., Wei, S., Li, C., et al. (2019). Comparative transcriptome analysis reveals resistance-related genes and pathways in *Musa acuminata* banana 'Guijiao 9' in response to Fusarium wilt. *Plant Physiology and Biochemistry* 141**,** 83-94. doi: 10.1016/j.plaphy.2019.05.022.

Sun, R.Z., Pan, Q.H., Duan, C.Q., and Wang, J. (2015). Light response and potential interacting proteins of a grape flavonoid 3 '-hydroxylase gene promoter. *Plant Physiology and Biochemistry* 97**,** 70-81. doi: http://dx.doi.org/10.1016/j.plaphy.2015.09.016.

Takahashi, A., Takeda, K., and Ohnishi, T. (1991). Light-Induced Anthocyanin Reduces the Extent of Damage to DNA in UV-Irradiated Centaurea cyanus Cells in Culture. *Plant Cell Physiology* 32(4)**,** 541-547. doi: 10.1093/oxfordjournals.pcp.a078113.

Tanaka, Y., Sasaki, N., and Ohmiya, A. (2008). Biosynthesis of plant pigments: anthocyanins, betalains and carotenoids. *The Plant Journal* 54(4)**,** 733-749. doi: https://doi.org/10.1111/j.1365-313X.2008.03447.x.

Tohge, T., de Souza, L.P., and Fernie, A.R. (2017). Current understanding of the pathways of flavonoid biosynthesis in model and crop plants. *Journal of Experimental Botany* 68(15)**,** 4013-4028.

Trewick, S.C., Henshaw, T.F., Hausinger, R.P., Lindahl, T., and Sedgwick, B. (2002). Oxidative demethylation by Escherichia coli AlkB directly reverts DNA base damage. *Nature* 419(6903)**,** 174-178. doi: https://doi.org/10.1038/nature00908.

Wall, M.M. (2006). Ascorbic acid, vitamin A, and mineral composition of banana (Musa sp.) and papaya (Carica papaya) cultivars grown in Hawaii. *Journal of Food Composition and Analysis* 19(5)**,** 434-445. doi: 10.1016/j.jfca.2006.01.002.

Wang, L., Tu, Y.-C., Lian, T.-W., Hung, J.-T., Yen, J.-H., and Wu, M.-J. (2006). Distinctive antioxidant and antiinflammatory effects of flavonols. *Journal of Agricultural and Food Chemistry* 54(26)**,** 9798-9804. doi: doi.org/10.1021/jf0620719.

Wen, W., Alseekh, S., and Fernie, A.R. (2020). Conservation and diversification of flavonoid metabolism in the plant kingdom. *Current Opinion in Plant Biology* 55**,** 100-108. doi: 10.1016/j.pbi.2020.04.004.

Winkel, B.S.J. (2006). "The biosynthesis of flavonoids," in *The Science of Flavonoids,* ed. E. Grotewold. (New York, USA: Springer Scienceand Business Media, Inc), 71-96.

Xu, F., Cheng, H., Cai, R., Li, L.L., Chang, J., Zhu, J., et al. (2008). Molecular cloning and function analysis of an anthocyanidin synthase gene from Ginkgo biloba, and its expression in abiotic stress responses *Molecules and Cells* 26(6)**,** 536-547.

Xu, F., Li, L., Zhang, W., Cheng, H., Sun, N., Cheng, S., et al. (2012). Isolation, characterization, and function analysis of a flavonol synthase gene from Ginkgo biloba. *Molecular Biology Reports* 39(3)**,** 2285-2296. doi: 10.1007/s11033-011-0978-9.

Yan, Y., Chemler, J., Huang, L., Martens, S., and Koffas, M.A. (2005). Metabolic engineering of anthocyanin biosynthesis in Escherichia coli. *Applied and Environmental Microbiology* 71(7)**,** 3617-3623.

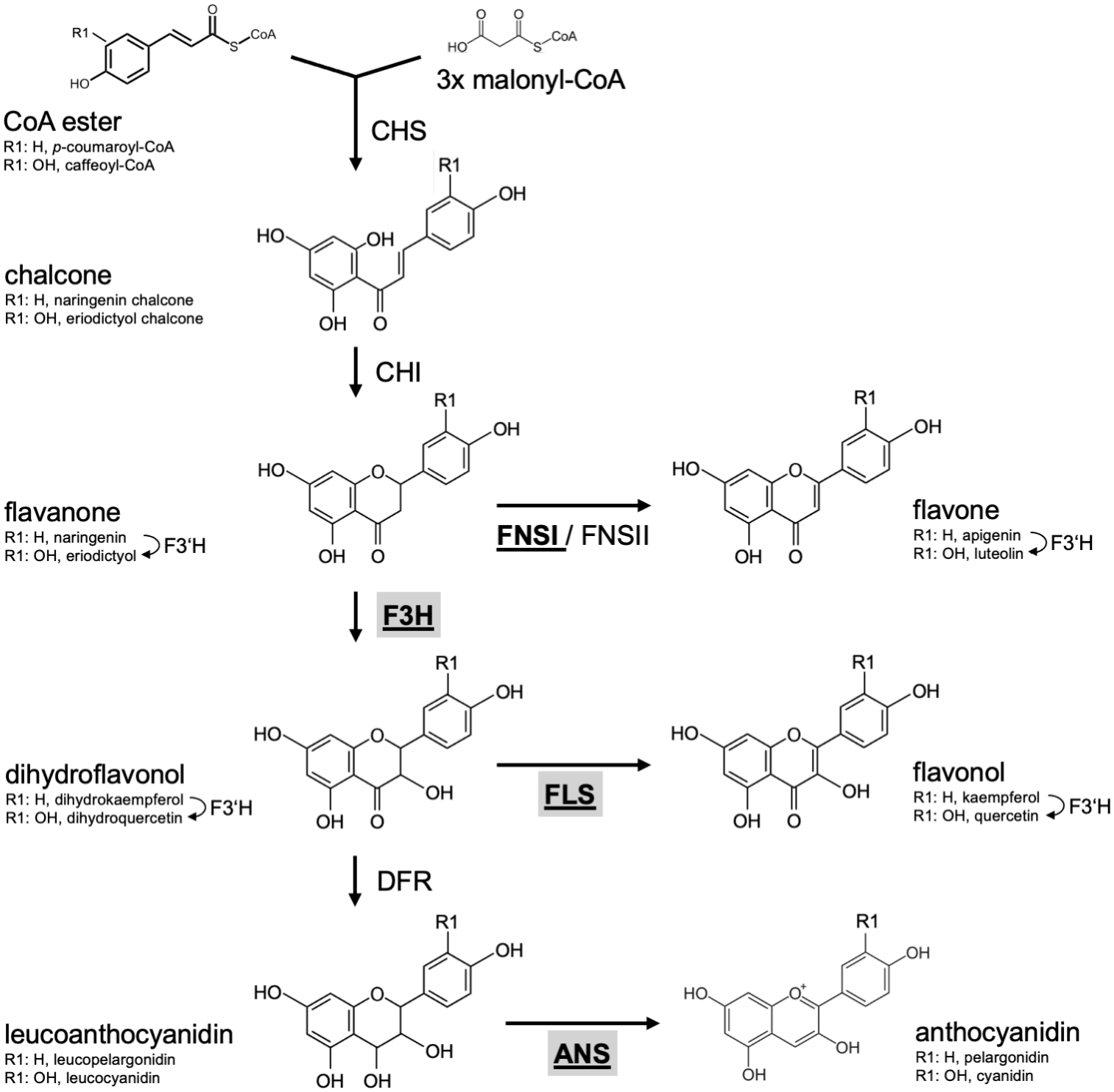

Figure 1: Schematic, simplified illustration of the core flavonoid aglycon biosynthesis pathway in plants.
Chalcone synthase (CHS), the first committed enzyme in flavonoid biosynthesis, connects a CoA ester and malonyl-CoA, forming a chalcone. Chalcone isomerase (CHI) introduces the heterocyclic ring. The resulting flavanone is converted to dihydroflavonol by flavanone 3-hydroxylase (F3H) or to flavones by flavone synthase (FNSI or FNSII). Dihydroflavonols are converted to flavonols by flavonol synthase (FLS). Alternatively, dihydroflavonol 4-reductase (DFR) can reduce dihydroflavonols to the corresponding leucoanthocyanidin, which is converted to anthocyanidin by the activity of anthocyanidin synthase (ANS). Flavonoid 3' hydroxylase (F3'H) hydroxylates 3' position of the B-ring using different flavonoid substrates. 2-oxoglutarate-dependant oxygenases are given in bold underlined. Enzymes in the focus of this work are highlighted by grey boxes.

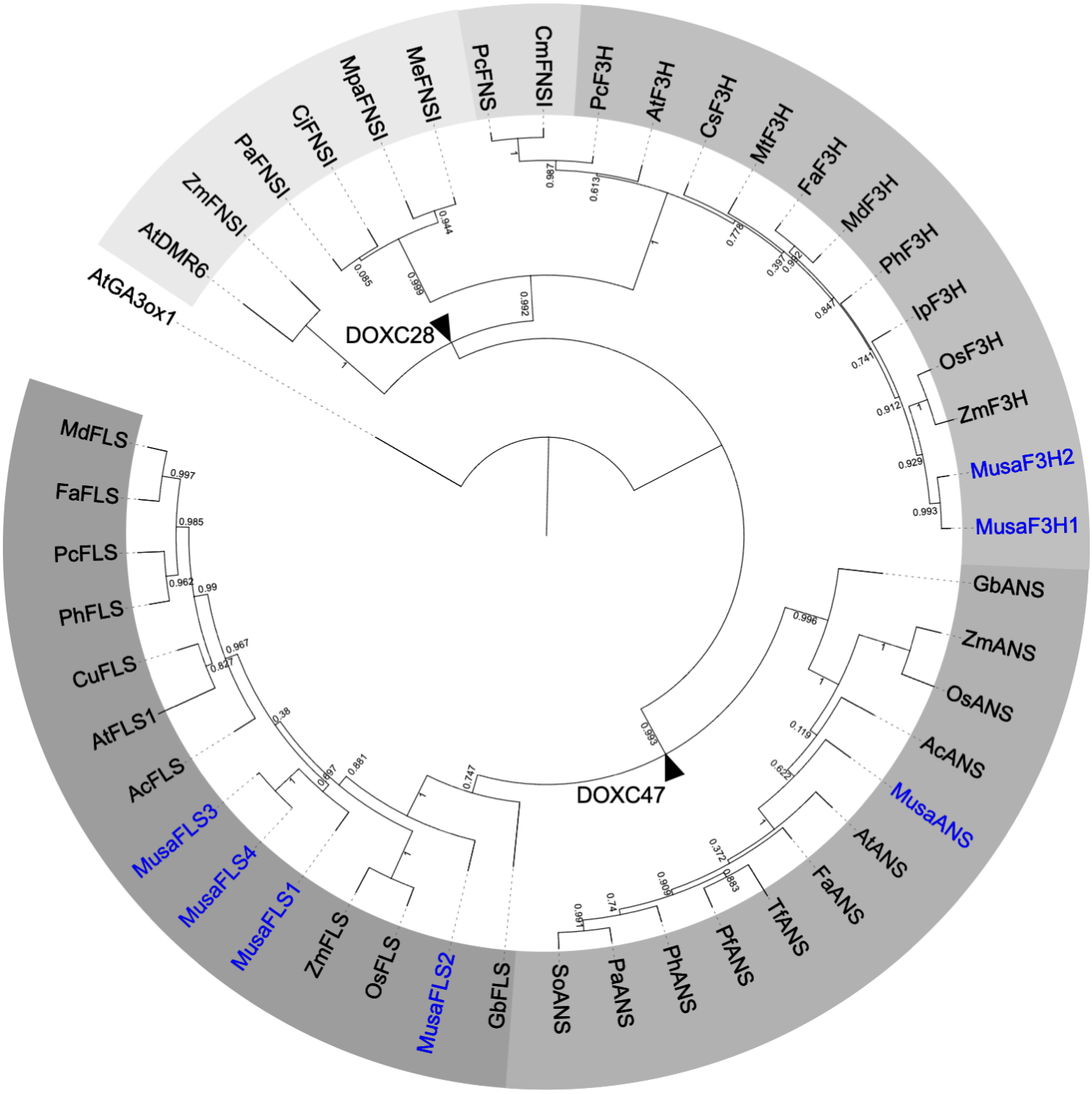

Figure 2: Rooted Approximately-Maximum-Likelihood (ML) phylogenetic tree of 2-ODDs involved in flavonoid biosynthesis.

ODDs from Banana are given in blue, 39 enzymes with proven F3H, FNSI, FLS or ANS activity were included. Different grey scales indicate F3H, FLS, ANS and two evolutionary FNSI clades. *At*GA3ox1 (gibberellin 3 beta-hydroxylase1) was used as an outgroup. Branchpoints to DOXC28 and DOXC47 classes are marked with black arrowheads.

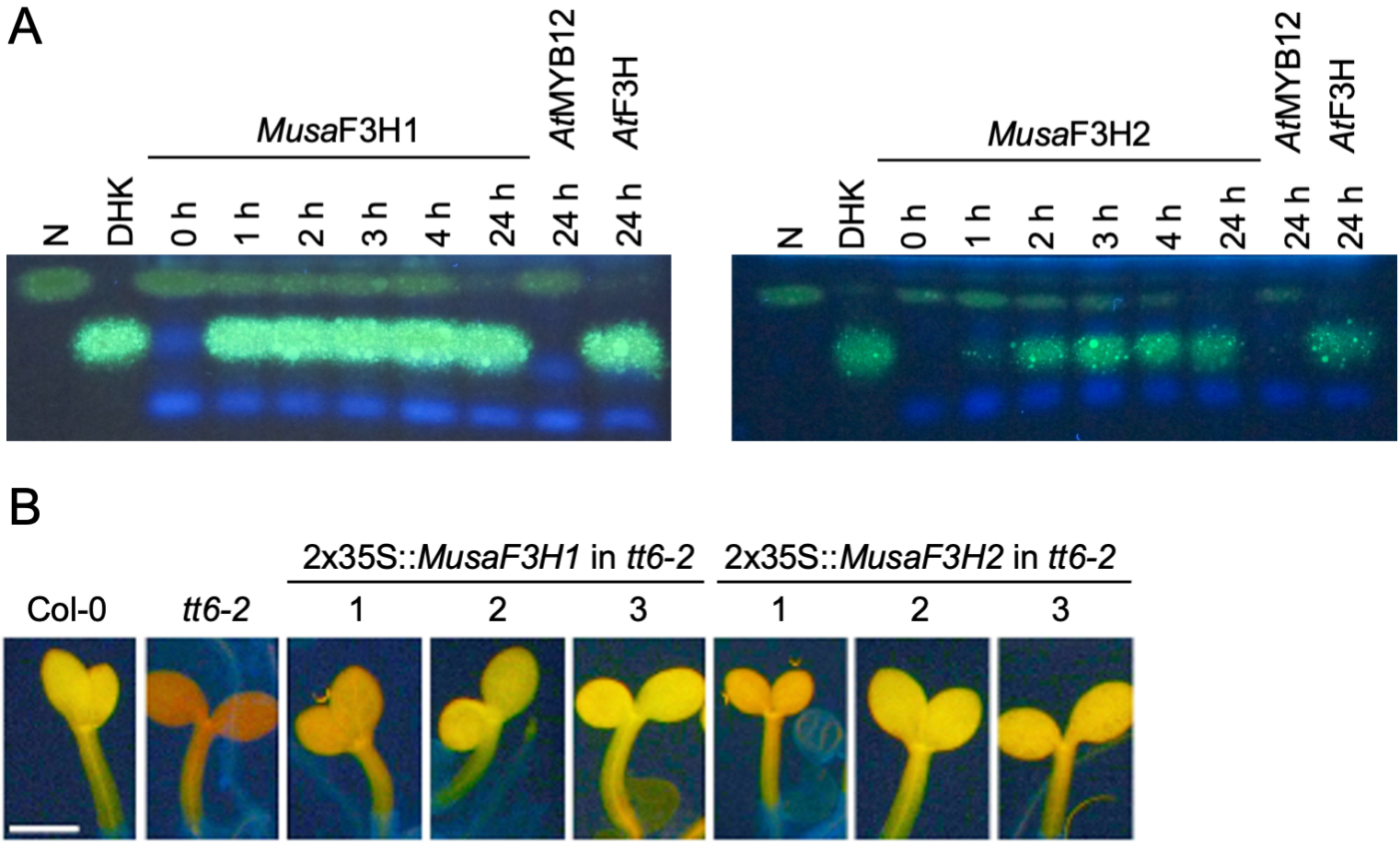

Figure 3: *Musa*F3H1 and *Musa*F3H2 are functional flavanone 3-hydroxylases.
(A) HPTLC analysis of F3H bioconversion assays using extracts from *E. coli* expressing recombinant *Musa*F3H1 or *Musa*F3H2. The substrate naringenin (N) and the product dihydrokaempferol (DHK) were used as standards. *At*F3H was used as a positive control. *At*MYB12 was used as a negative control. (B) Analysis of *tt6-2* mutant seedlings complemented with *Musa*F3H1 and *Musa*F3H2. Col-0 wildtype and *tt6-2* were used as controls. Representative pictures of DPBA-stained seedlings under UV light are given. Yellow fluorescence indicates flavonol glycoside accumulation. The different numbers indicate individual transgenic lines. The scale bar indicates 0.5 mm.

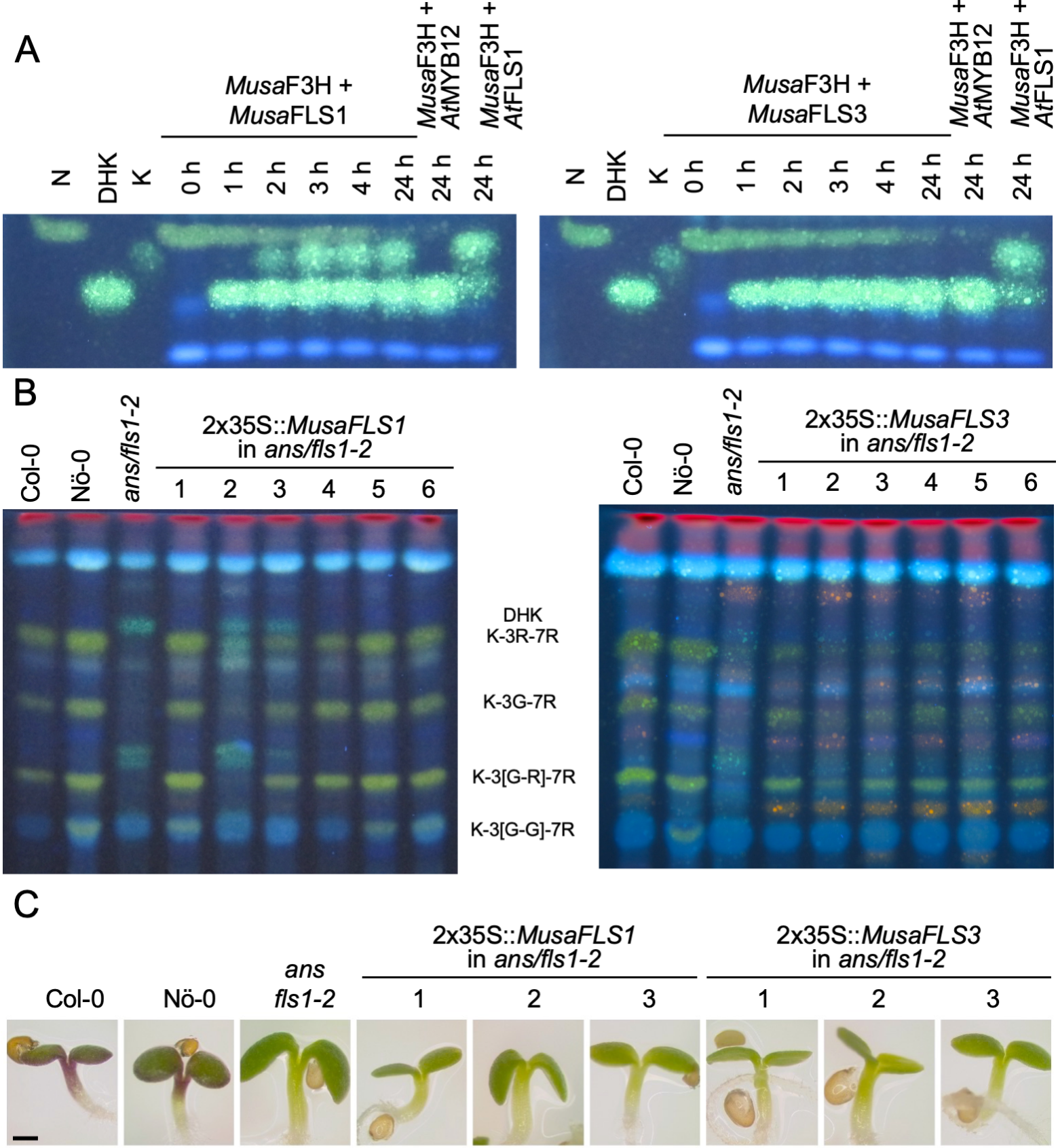

Figure 4: *Musa*FLS1 and *Musa*FLS3 are functional flavonol synthases.
(A) HPTLC analysis of a FLS bioconversion assays using extracts from *E. coli* expressing recombinant *Musa*FLS1 or *Musa*FLS3. The F3H substrate naringenin (N), the FLS substrate dihydrokaempferol (DHK) and the product kaempferol (K) were used as standards. *At*FLS1 served as a positive control and *At*MYB12 was used as a negative control. (B) Flavonol glycoside accumulation in *Musa*FLS-complemented *ans/fls1-2* seedlings, analysed by HPTLC analysis. Col-0, Nö-0 (both wildtype) and *ans/fls1-2* were used as controls. Bright green spots belong to derivates of kaempferol, orange spots are derivates of quercetin and faint blue shows sinapate derivatives. Dark green and yellow spots indicate DHK and DHQ, respectively. G, glucose; K, kaempferol; Q, quercetin; R, rhamnose (C) Representative pictures of anthocyanin (red) accumulation in 6-day-old *Musa*FLS-complemented *ans/fls1-2* seedlings growing on 4 % sucrose. The scale bar indicates 0.5 mm.

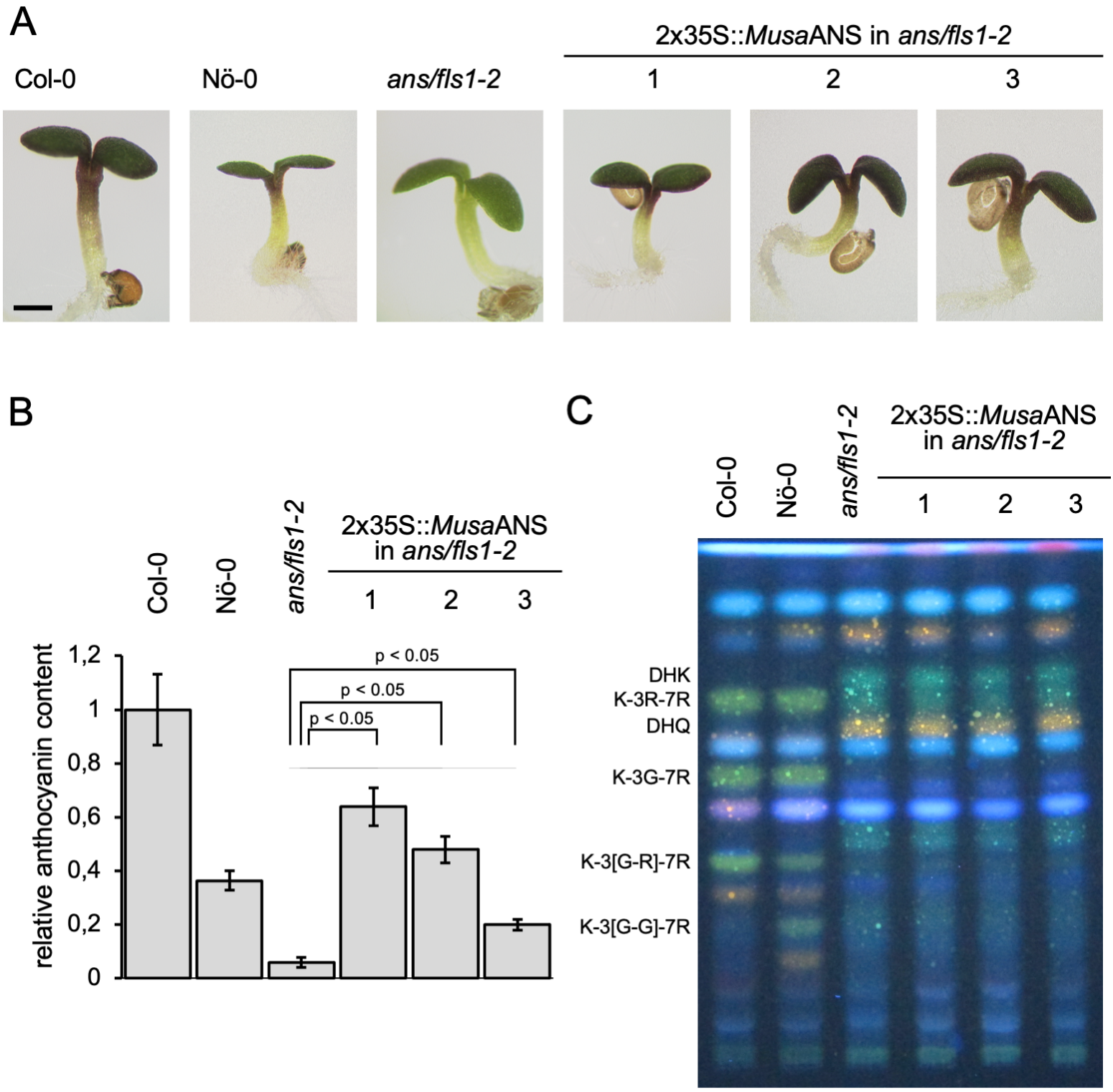

Figure 5: *Musa*ANS is a functional anthocyanin synthase.
Analysis of *ans/fls1-2* double mutant seedlings complemented with 2x35S driven *MusaANS* demonstrate *in planta* ANS functionality of *Musa*ANS by anthocyanin accumulation. The different numbers indicate individual transgenic lines. (A-B) Sucrose induced anthocyanin accumulation in 6-day-old *A. thaliana* seedlings. (A) Representative pictures of seedlings (the scale bar indicates 0.5 mm) and (B) corresponding relative anthocyanin content. Error bars indicate the standard error for three independent measurements. (C) *Musa*ANS does not show *in planta* FLS activity. Flavonol glycoside accumulation in *MusaANS*-complemented *ans/fls1-2* seedlings, analysed by HPTLC analysis. Col-0, Nö-0 (both wildtype) and *ans/fls1-2* were used as controls. Bright green spots belong to derivates of kaempferol, orange spots are derivates of quercetin and faint blue shows sinapate derivatives. Dark green and yellow spots indicate DHK and DHQ, respectively. G, glucose; K, kaempferol; Q, quercetin; R, rhamnose.